NOAA Technical Memorandum ERL WPL-131

INFRASOUND FROM DISTANT ROCKET LAUNCHES

Gary E. Greene
A. J. Bedard, Jr.

Wave Propagation Laboratory
Boulder, Colorado
February 1986

noaa NATIONAL OCEANIC AND ATMOSPHERIC ADMINISTRATION / Environmental Research Laboratories

NOAA Technical Memorandum ERL WPL-131

INFRASOUND FROM DISTANT ROCKET LAUNCHES

Gary E. Greene
A. J. Bedard, Jr.

Wave Propagation Laboratory
Boulder, Colorado
February 1986

UNITED STATES
DEPARTMENT OF COMMERCE

Malcolm Baldrige,
Secretary

NATIONAL OCEANIC AND
ATMOSPHERIC ADMINISTRATION

Anthony J. Calio,
Administrator

Environmental Research
Laboratories

Vernon E. Derr,
Director

NOTICE

Mention of a commercial company or product does not constitute an endorsement by NOAA Environmental Research Laboratories. Use for publicity or advertising purposes of information from this publication concerning proprietary products or the tests of such products is not authorized.

CONTENTS

INFRASOUND FROM DISTANT ROCKET LAUNCHES

Gary E. Greene[1]

A. J. Bedard Jr.

ABSTRACT

From 1959 through 1969 low-frequency (0.02-1.0 Hz) acoustic signals related to missile launches from Cape Canaveral were recorded by an infrasonic station in Washington, DC. Although the characteristics of these signals are considerably more variable than those from other known sources, the acoustic signatures can resemble those from sources both natural and man-made. A general summary includes 61 missile-related signals with specific examples of their features.

1. INTRODUCTION

From the late 1940's to 1971 an infrasonic station in Washington, DC, continuously recorded pressure fluctuations from 0.001 to 1.0 Hz for the purpose of detecting acoustic waves (infrasound) from natural and man-made sources. Infrasound occurs from a great variety of atmospheric sources. It is a challenge to identify methods of distinguishing the various source mechanisms from the detailed character of the far-field acoustic signatures. Distin-

---

[1]Cooperative Institute for Research in the Environmental Sciences, University of Colorado, Boulder, Colorado 80303.

guishing features have been identified for some sources such as geomagnetic activity (Chrzanowski et al., 1961) and earthquakes (Bedard, 1971; Young and Greene, 1982); for other sources, additional studies seem necessary to determine unique features. Infrasound measurements from the vicinity of geophysical sources have proved difficult to identify from the far-field acoustic signature alone. Although many of these sources can be well-characterized from their statistics or comparisons with independent data (e.g., meteor sightings [Bedard and Greene, 1981]), in a given situation dominant, identifying features (such as duration) may be masked by noise or be nonexistent. Acoustic energy from severe weather (Bowman and Bedard, 1971; Georges, 1973), volcanic explosions (Goerke et al., 1965), or the vicinity of mountains (Bedard, 1978) seems to have few unique acoustic features. Cook (1962), Cook and Young (1962), and Greene and Howard (1975) have reviewed properties of natural infrasound.

The characteristics of infrasound related to missile launches are much more variable than those from any other known source and are much more difficult to classify. A number of investigators have published studies of long range infrasound from missile launches. Donn et al. (1968), Kaschak (1969), and Kaschak et al. (1970) reviewed measurement techniques, some case studies, and statistical properties in a passband of about .1 Hz to higher frequencies. Multiple arrivals from both the launch and reentry region were noted in these studies which also found evidence of strong propagation effects on the measured waves. Kaschak et al. (1970) and Balachandran et al. (1971) concluded that infrasound generated aerodynamically (as opposed to the initial rocket firing) was detected at long distances. More recently Donn et al.

(1975) addressed propagation effects in more detail, finding that summer signals tend to have more low-frequency content than winter signals do. Tahira and Donn (1983) provided strong evidence for the aerodynamic generation of sound during booster reentry.

To distinguish missile-related infrasound from other types of infrasound, we analyzed the infrasonic signatures of 61 missile signals. All the data included herein are from signals recorded at Washington, DC, from missile launches at Cape Canaveral, Florida.

2. EQUIPMENT AND ANALYSIS PROCEDURE

The recording station at Washington (Cook and Bedard, 1971) consisted of four microphones spaced 5 to 7 km apart in a quadrilateral. The signal from each microphone was transmitted over telephone lines to the laboratory and recorded on analog magnetic tape. Graphic recordings were reproduced from the tape and electronically filtered to give the passband shown in Fig. 1. These records were visually cross-correlated to yield azimuth and horizontal phase velocity (trace velocity) along the Earth's surface from time differences of arrival of points of equal phase at the microphones. For most signals we believe the azimuth to be accurate to ±2°, the trace velocity to ±10 m/s.

The determination that a signal was missile-related required both an arrival time from 60 to 80 minutes after a known launch time and an azimuth of arrival between 170 and 200 degrees. The distance and azimuth to Washington from the Cape are about 1215 km and 196 degrees. Our signals average 69.0 min travel time to the first recognizable correlation (start time) and 189.8

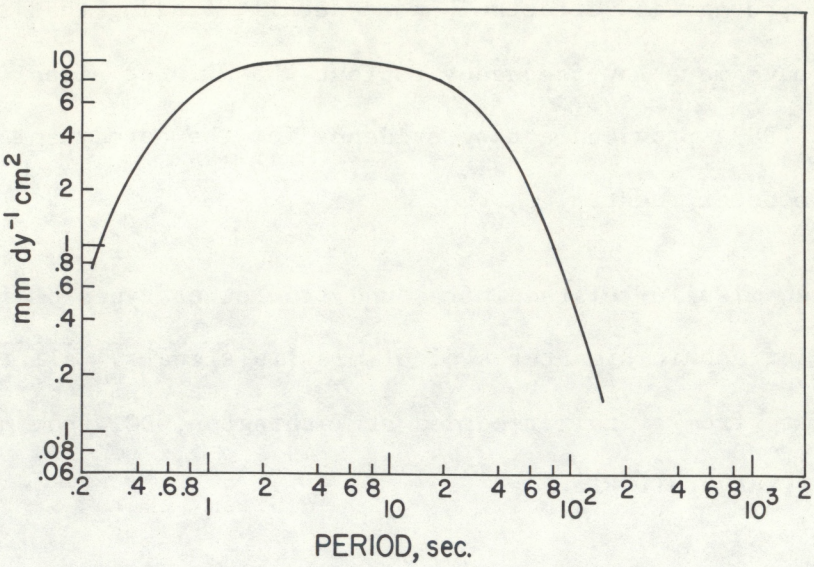

Figure 1. Passband of microbarograph system.

degrees azimuth. The former is consistent with generally accepted travel speeds, but the latter suggests a source different from the launch pad location. More is said of this in Section 4.

3. SIGNAL CHARACTERISTICS

The large variability of these signals precludes the showing of a typical example. However, all the signals are composed of one or more of five characteristics defined for the purpose of this report:

1) High-frequency--periods up to 10 s.
2) Middle-frequency--periods from 10 to 20 s.
3) Low-frequency--periods greater than 20 s.
4) Pulse--a distinct and usually abrupt isolated wave of any frequency.
5) Burst--a short-lived train of distinct, nearly monochromatic, high frequency waves.

These definitions are somewhat arbitrary, but Fig. 2 illustrates them. The figures are an overlay of only two traces aligned for best correlation for purposes of clarity. Analysis uses all four traces.

Figure 2a shows a signal containing only "high frequency" energy. Although 33 of the 61 total signals contain these frequencies only 5 were lacking any of the other characteristics. A typical example of a "middle-frequency" arrival is shown in Fig. 2b. This range is contained in 41 signals, 10 of them exclusively. The "low frequencies" shown in Fig. 2c usually occur near the end of an arrival whose maximum energy is contained at shorter periods. Occasionally, as in this example, thse longer periods dominate the entire signal in which higher frequency components show a much reduced amplitude. In 34 cases, periods longer than 20 s appeared but only twice without some other feature. Figure 2d is an excellent example of a late arriving pulse. Signal began at 0347 and ended near 0402, with some low-frequency energy showing in the figure. Three minutes later a pulse, about 3 times more energetic than anything else in the signal, appeared abruptly. One or more pulses was present in 21 of our arrivals but never alone. Figure 2e shows a "burst" of about 3 s period energy occurring more than 3 min after signal onset in the midst of longer periods. This characteristic was observed in only six signals and never alone. Figure 2f shows perhaps the closest thing to a typical missile signal. Most of the energy is at higher frequencies early and becomes lower with time. A pulse, although occurring more often near the end of a signal, is seen standing out in the middle of this example.

The Appendix lists all 61 missile-related signals and includes details of frequency, amplitude, azimuth, and trace velocity. Launch time and, where possible, the launch name and booster are also given.

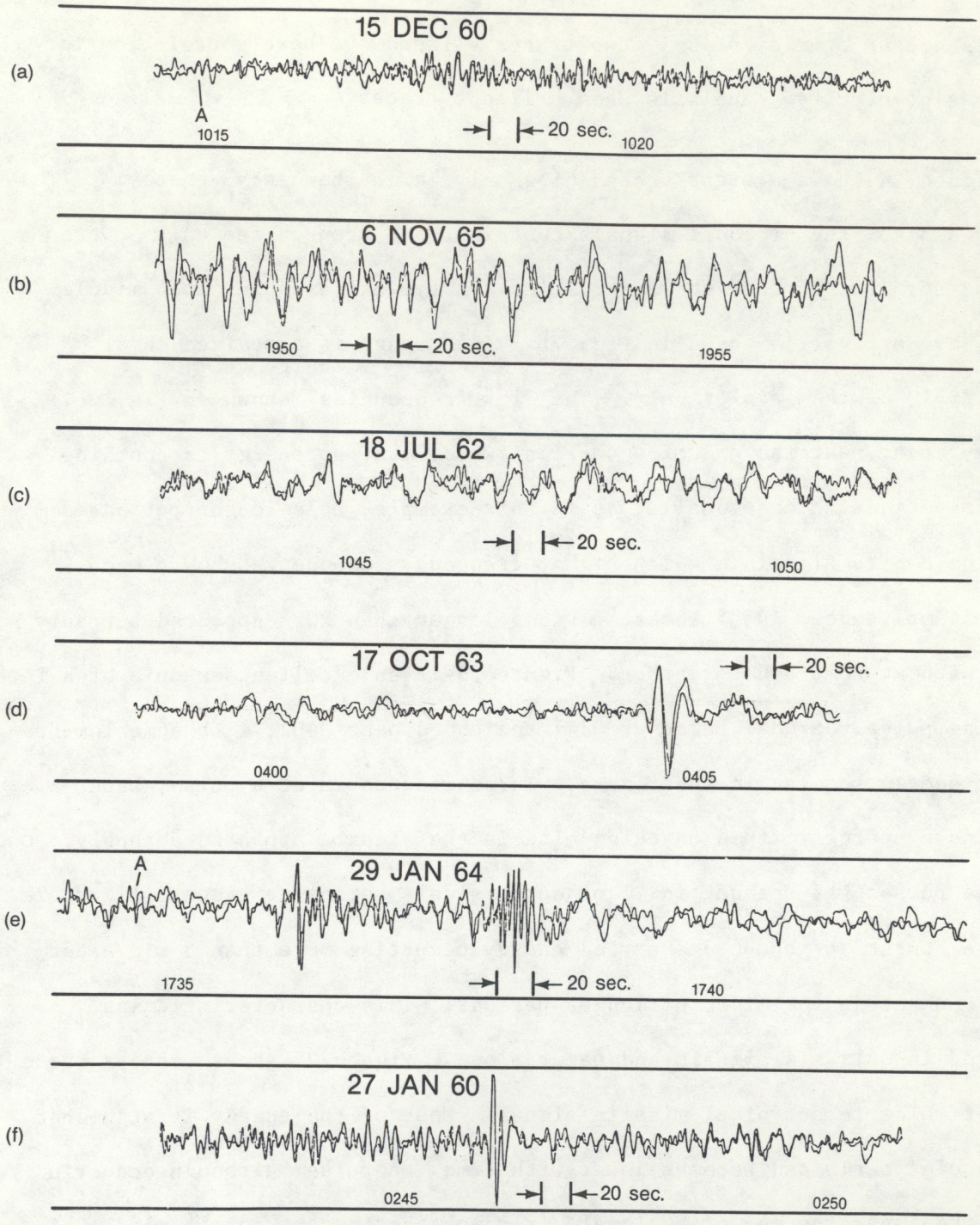

Figure 2. Examples of the various signal types detected from missile launches.

Missile signatures in which a significant change in frequency with time occurs are nearly always from shorter to longer periods. Of 33 total signals showing large frequency changes, 26 had shorter periods at the onset. Only four began with longer periods and ended at higher frequencies; three were more complex and went in both directions.

Besides the 61 signals included herein, 23 others are probably missile related, but we were unable to determine a launch time even though there was a launch on the same day. Five others are possible but no launch could be verified on those days. All 28 of these signals are from the correct direction and exhibit the same general characteristics as the known signatures. None of these data were used in this report.

There were also 65 known launches for which we were operational but found no signals. Noisy background conditions were responsible for only part of this number. Table 1 shows the distribution of the background noise conditions during the expected time of arrival from known launches that were not detected and the distribution of the maximum amplitude, including pulses, of the known detections. Our failure to detect 54% of the launches whose expected arrival time occurred when the background was not greater than 1 dyn/cm^2 is most likely due to unfavorable propagation conditions or some feature of the missile itself that resulted in a weak acoustic generation process.

Table 1. Summary of Signal Statistics

	Amplitude (dyn/cm^2, zero-to-peak)			
	0.1-0.5	0.6-1.0	1.1-2.0	>2.0
Signals detected	20	19	14	8
(%)	(33)	(31)	(23)	(13)
Signals not detected	24	11	12	18
(%)	(37)	(17)	(18)	(28)

4. STATISTICS

Figure 3 indicates the range of signal periods and horizontal trace speeds measured for these events. There seems no clear relationship between period and trace speed. However the presence of many signals with trace speeds higher than 360 m s^{-1} provides one means of distinguishing this type of signal from surface explosions at similar distances. Acoustic energy from distant explosions usually travels with a horizontal trace speed near 340 m s^{-1}. Although acoustic signals related to geomagnetic activity show such high speeds, the typical durations for such signals (hours), and the fact that systematic azimuth/time variations occur offer means of distinguishing geomagnetically related acoustic signals from those related to missile launches.

Figure 4 is a plot of maximum signal amplitude as a function of period. Except for a tendency for some of the larger amplitudes to occur at smaller periods, there does not seem to be a clear trend in the data. Most signals were detected with pressure levels less than 2 μb (0-peak).

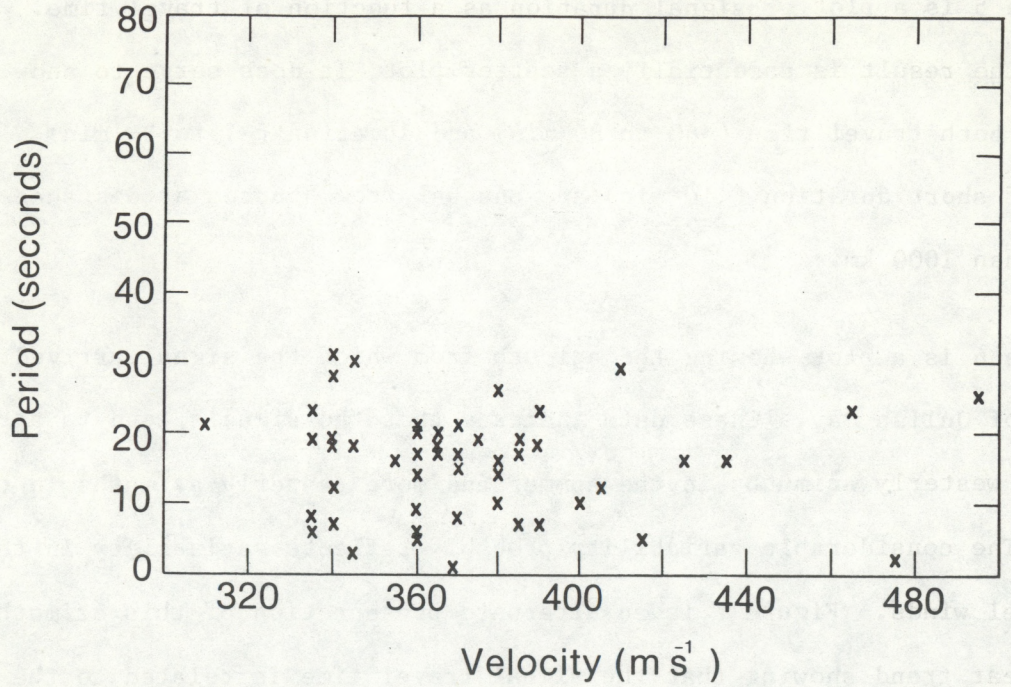

Figure 3. Signal period as a function of horizontal phase velocity.

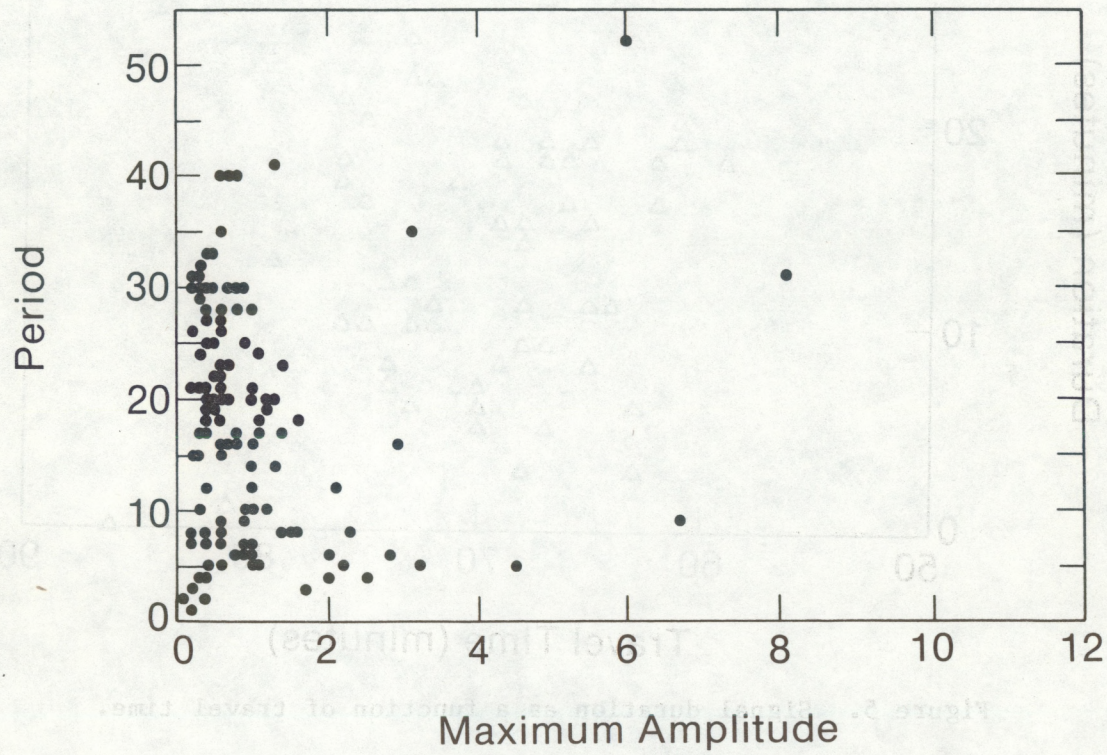

Figure 4. Maximum signal amplitude as a function of period.

Figure 5 is a plot of signal duration as a function of travel time. Although the result is essentially a scatter plot, it does serve to show the bounds of both travel time (~60 to 80 min) and duration (~1 to 30 min). The signals of short duration (<10 min) are unusual from sources at distances greater than 1000 km.

Figure 6 is a plot showing the azimuth from which the signal arrived as a function of Julian day. These data indicate that the signals tend to arrive from more westerly azimuths in the summer and more easterly azimuths in the winter. The considerable variability probably reflects variability in the upper level winds. Figure 7 is an alternate presentation of this azimuth/time-of-year trend showing that the signal travel time is related to the path

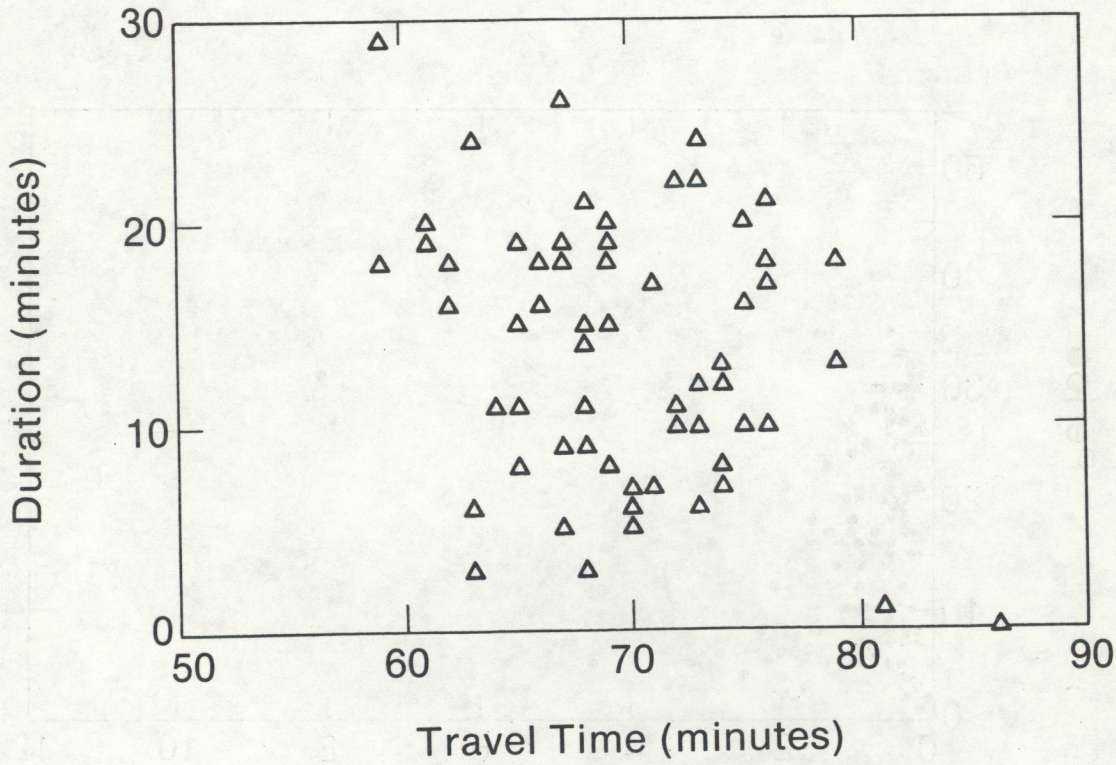

Figure 5. Signal duration as a function of travel time.

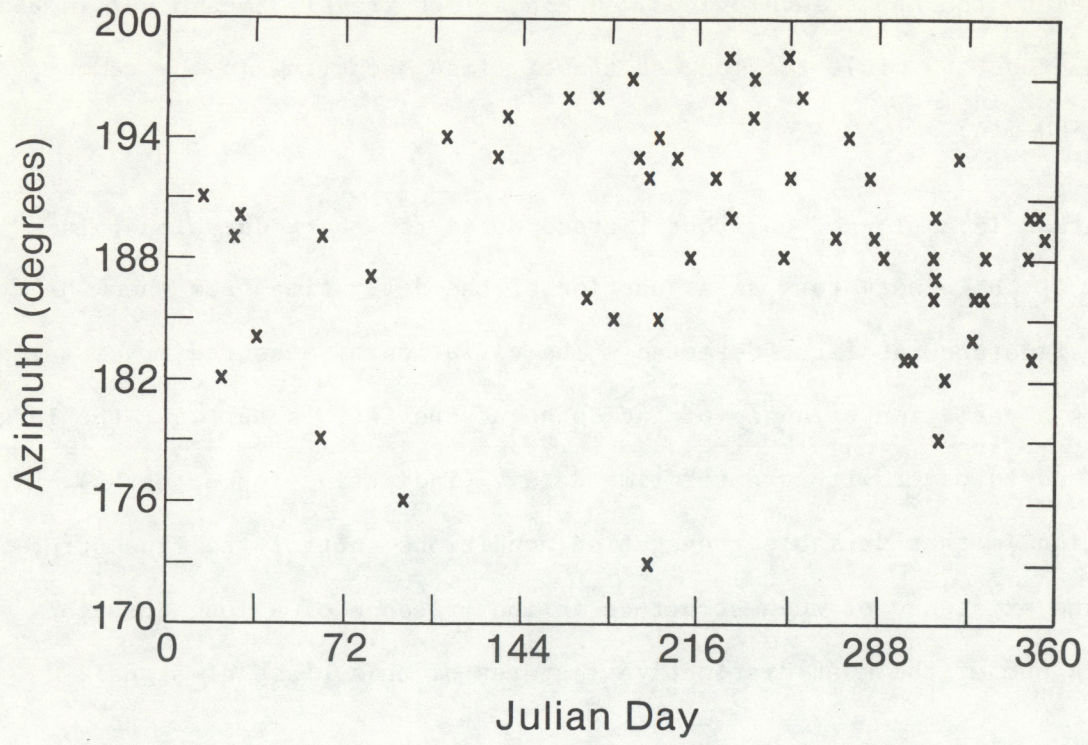

Figure 6. Signal azimiuth as a function of Julian day.

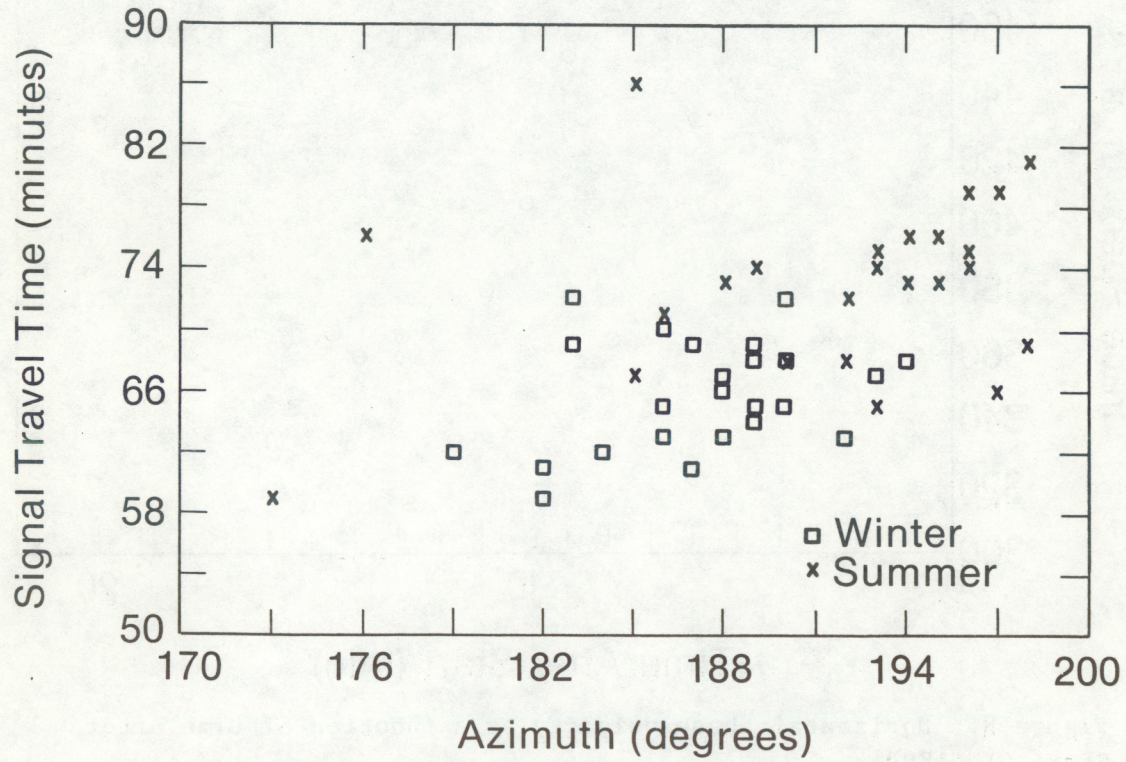

Figure 7. Signal azimuth as a function of travel time.

controlled by the upper level winds. The smallest travel times occur in the winter months (~60 min), the longest travel times occurring in the summer months (~80 min).

Figure 8 is a plot of horizontal trace speed for short duration pulses measured at the observatory as a function of the delay time from when the missile signature was first detected. The variation of measured trace speed indicates a variation of angle of incidence at the Earth's surface; the larger angles tend to occur with greater time delays (indicating longer paths). The implication is that variable propagation conditions control the fine structure. The existence of such structure in the presence of a long duration signal is one of the most distinctive features of this class of signal.

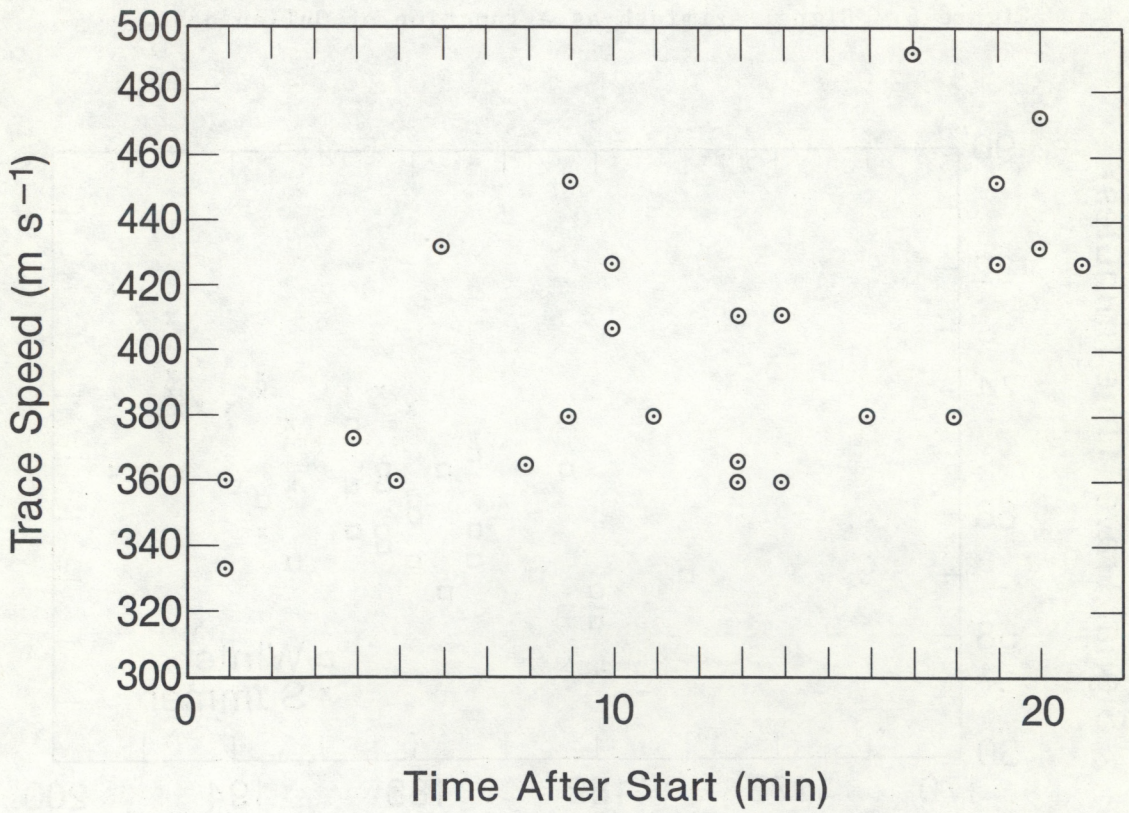

Figure 8. Horizontal phase velocity as a function of time after start of signal.

The actual source of acoustic energy detected 1200 km away is still in question. We have two pieces of evidence that argue against the launch site itself as the origin. First, we were never able to detect any signals from several static firings of very powerful boosters at Huntsville, Ala., during the early 1960's even though the distance was less and we operated several times during very favorable noise conditions. Also the average azimuth of 61 signals was 189.8°, nearly 6° or approximately 125 km east from the launch pad location. The prevailing upper winds (westward in winter, eastward in summer) are not responsible for this difference (Georges and Beasley, 1971; Georges, 1971). The 33 signals received between mid-September and mid-March averaged 187.6°, and the summer average of signals was 192.2°. These numbers are consistent with a 2° to 3° azimuth shift, which would be expected on average because of the winds. These data suggest that the infrasound source is generated downrange, perhaps when the missile reaches supersonic speeds. This is in agreement with earlier conclusions (e.g., Balachandran et al., 1971).

5. CONCLUDING REMARKS

We have provided statistics defining properties of measured far-field acoustic signatures from missile launches. Because we were unable to obtain details concerning launch characteristics (e.g., thrust, launch angle) we have not compared the far-field signals with launch details. We hope that this report may also serve as a basis for performing such a comparison.

Properties of the signatures provide information on long-range propagation effects. For example, Figs. 6 and 7 indicate the effects of the propagation path upon the azimuth-of-arrival, which varies over a range from about 182 to

198°. Also properties such as duration, period, and amplitude can be used to characterize this signal type. The feature most valuable in distinguishing between these signatures and signatures from other sources is the frequent occurrence of fine-structure in the form of impulsive regions of acoustic energy. A possible explanation of these pulse signatures occurring in a longer duration signal is the highly selective launching of acoustic energy by a missile bow wave. Highly directional acoustic energy in the source region could select one of a number of possible propagation paths.

6. REFERENCES

Balachandran, N. K., W. L. Donn, and G. Kaschak, 1971. On the propagation of infrasound from rockets: Effects of winds. J. Acoust. Soc. Am. 50:397-404.

Balachandran, N. K., and W. L. Donn, 1971. Characteristics of infrasonic signals from rockets. Geophys. J. R. Astron. Soc. 26:135-148.

Bedard, A. J. Jr., 1971. Seismic response of infrasonic microphones. J. Res. Natl. Bur. Stand. 75C:41-45.

Bedard, A. J. Jr., 1977. The d-c pressure summator: Theoretical operation, experimental test and possible practical uses. Fluidics Quart. 9:26-51.

Bedard, A. J. Jr., 1978. Infrasound originating near mountainous regions in Colorado. J. Appl. Meteorol. 17:1014-1022.

Bedard, A. J. Jr., and G. E. Greene, 1981. Case study using arrays of infrasonic microphones to detect and locate meteors and meteorites. J. Acoust. Soc. Amer. 69:1277-1279.

Bowman, H. S., and A. J. Bedard, 1971. Observations of infrasound and subsonic disturbances related to severe weather. Geophys. J. Roy. Astrom. Soc. 26:215-242.

Chrzanowski, P., G. Greene, K. T. Lemmon, and J. M. Young, 1961. Traveling pressure waves associated with geomagnetic activity. J. Geophys. Res. 66:3727-3733.

Cook, R. K., 1962. Strange sounds in the atmosphere. 1. Sound 1:12-16.

Cook, R. K., and J. M. Young, 1962. Strange sounds in the atmosphere. 2. Sound 1:25-33.

Cook, R. K., and A. J. Bedard, 1971. On the measurement of infrasound. Geophys. J. R. Astron. Soc. 26:5-11.

Donn, W. L., E. Posmentier, U. Fehr, and N. K. Balachandran, 1968. Infrasound at long range from Saturn V, 1967. Science 162:1116-1120.

Donn, W. L., N. K. Balachandran, and D. Rind, 1975. Tidal wind control of long-range rocket infrasound. J. Geophys. Res. 80:1662-1664.

Georges, T. M., 1971. A program for calculating three-dimensional acoustic-gravity ray paths in the atmosphere. NOAA Tech. Rep. ERL 212-WPL 16, NOAA Environmental Research Laboratories, Boulder, Colo., 43 pp.

Georges, T. M., 1973. Infrasound from convective storms: Examining the evidence. Rev. Geophys. Space Phys. 11:571-594.

Georges, T. M., and W. H. Beasley, 1977. Refraction of infrasound by upper-atmospheric winds. J. Acoust. Soc. Am. 61:28-34.

Goerke, V. H., J. M. Young, and R. K. Cook, 1965. Infrasonic observations of the May 16, 1963, volcanic explosion on the Island of Bali. J. Geophys. Res. 70:6017-6022.

Greene, G. E., and J. Howard, 1975. Natural infrasound: A one-year global study. NOAA Tech. Rep. ERL 317-WPL 37, NOAA Environmental Research Laboratories, Boulder, Colo., 153 pp.

Kaschak, G. R., 1969. Long-range supersonic propagation of infrasonic noise generated by missiles. J. Geophys. Res. Space Phys. 74:914-918.

Kaschak, G., W. Donn, and U. Fehr, 1970. Long-range infrasound from rockets. J. Acoust. Soc. Am. 48:12-20.

Tahira, M., and W. L. Donn, 1983. Anomalous infrasound from Space Shuttle II and Skylab I. J. Acoust. Soc. Am. 72:461-464.

Young, J. M., and G. E. Greene, 1982. Anomalous infrasound generated by the Alaskan earthquake of 28 March 1964. J. Acoust. Soc. Am. 71:334-339.

APPENDIX A. Signal Properties

Date	Start Time (UT)	Interval	Period (s)	Max. Ampl. Zero-peak (dyn/cm^2)	Az (deg)	Vel. (m/s)	Launch			
							Name	Booster	Time (UT)	Signal Travel Time (min)
3 /3 /59	0618	0618-0621	6-8	0.6			Pioneer IV	Juno II	0511	67
		0621-0627	10-12	1.0	179	340				
8 /15/59	0152	0153*	21	1.0	198	360	Beacon	Juno II	0031	81
		0154	15	0.5						
9 /9 /59	0832	0832-0835	5-8	0.2			Big Joe	Atlas	0719	73
		0835-0844	11-17	1.1	192	360				
10/29/59	0321	0321-0328	19-23	0.6	183	335		Thor	0212	69
		0328-0336	11-15	0.6	187	370				
11/26/59	0831	0831-0835	2-7	1.0	186	340	Pioneer	Atlas	0726	65
		0835-0846	20-25	0.5						
12/17/59	0111	0111-0112	1-2	0.1	201	475		Thor	0003	68
		0113-0114	1	0.2	187	369				
1 /14/60	1746	1746-1751	16-19	0.5				Thor	1135	71
		1751-1753	8-10	1.2	191	400				
		1753-1803	18-22	0.6						
1 /27/60	0240	0240-0248	6-9	0.6						
		0246*	6	2.8	189	360		Atlas	0131	69
		0248-0259	15-20	0.7						
5 /13/60	1030	1030-1042	14-21	0.3	193	370	Echo	Delta	0916	74
6 /11/60	0745	0745-0751	20-27	0.4						
		0749-0801	10-17	0.8	196	370		Atlas	0630	75
		0800*	20	0.7						
8 /12/60	1054	1054-1100	13-19	0.4	196	375	Echo I	Delta	0940	74
		1100-1107	23-31	0.3						
9 /28/60	1543	1543-1552	12-17	0.3	193	385		Titan	1438	65
		1554-1602	20-24	0.3						
10/13/60	1043	1043-1058	12-20	0.6	189	360	Air Force	Atlas	0935	68
		1044-1051	4-9	0.6						
11/23/60	1216	1216-1219	14-18	0.4	186	340	Tiros II	Delta	1113	63
12/15/60	1015	1015-1023	3-9	0.9	190	360	Pioneer	Atlas	0910	65
6 /23/61	0420	0420-0438	17-30	0.5	196	345		Atlas	0301	79
7 /7 /61	0610	0610-0623	13-18	0.6	197	390	Disc 26		0451	79
9 /13/61	1518	1518-1526	22-30	0.7			Mercury	Atlas	1404	74
		1521-1522	10-14	1.0	196	360				
10/2 /61	1931	1931-1940	3-7	0.9	194	390	Air Force	Atlas	1823	68
11/22/61	2218	2218-2225	10-15	0.2				Atlas	2103	75
		2227*	14	1.3	181	380				
		2228-2233	21-23	0.7	188	390				
		2238*	16	0.7	184	435				
7 /10/62	0950	0950-1000	17-19	0.4	193	335	Telstar	Delta	0835	75
7 /18/62	1043	1043-1053	23-28	0.6	194	340	Echo	Thor	0930	73
		1045-1050	12-15	0.3						
11/16/62	1852	1852-1857	12-16	2.9	193	355		Saturn	1745	67

APPENDIX (Continued)

Date	Start Time (UT)	Interval	Period (s)	Max. Ampl. Zero-peak (dyn/cm^2)	Az (deg)	Vel. (m/s)	Launch			
							Name	Booster	Time (UT)	Signal Travel Time (min)
6 /19/63	1101	1101-1110	21-29	0.3	186	410	Tiros III	Delta	0950	71
		1118*	25	0.9	195	495				
7 /26/63	1549	1549-1556	4-7	0.2			Syncom II	Delta	1433	76
		1553-1606	15-21	0.6						
		1557*	17	1.4	193	365				
10/17/63	0347	0347-0402	10-21	0.3	188	310	Air Force	Atlas	0240	67
		0405*	16	1.0	187	380				
11/27/63	2009	2009-2016	3-7	0.4	188	385	Centaur	Atlas	1903	66
		2015-1025	12-20	0.5	187	365				
		2023*	30	0.4						
1 /29/64	1735	1735-1738	3-5	0.6			Saturn V	Saturn	1625	70
		1736*	6	2.0	190	335				
		1738-1739	3	1.7	190	345				
		1739-1742	22-30	0.3						
8 /25/65	1633	1633-1642	5-10	0.3	195	380	Oso-C	Delta	1517	76
		1639-1643	15-21	0.2						
11/6 /65	1949	1949-1955	14-18	0.6	186	365	Expl XXIX	Delta	1839	70
12/15/65	1444	1444-1446	2-3	0.2			Gemini-6	Titan	1337	67
		1446-1451	5-8	0.4	188	335				
		1449-1458	11-17	0.4						
		1457-1503	24-31	0.3	179	340				
12/16/65	0843	0843-0854	13-19	0.5	183	340	Pioneer VI	Delta	0731	72
		0847-0850	28-32	0.3						
5 /17/66	1628	1628-1644	12-19	1.2	195	385	Gemini	Atlas	1515	73
		1633-1638	23-30	0.9						
		1644-1652	19-22	0.5						
		1650*	23	1.4	195	465				
8 /10/66	2034	2034-2038	3-5	0.4	192	360	Lunar Orbiter I	Atlas	1926	68
		2938-2048	12-15	0.5						
8 /25/66	1822	1822-1828	4-8	1.5	197	370	Apollo 3	Saturn	1716	66
		1828-1840	20-35	0.6						
10/27/66	0014	0014-0032	9-18	1.1	183	345	Intelsat II	Delta	2305	69
11/7 /66	0029	0029*	8	1.5	190	335	Lunar Orbiter II	Atlas	2321	68
		0030-0032	3-8	1.6						
		0040-0046	22-25	0.4						
		0050*	16	0.8	177	425				
11/11/66	2007	2007	2-5	1[1]	182	415	Gemini XII	Atlas	1908	59
		2007-2013	3-6	1						
		2013-2017	10-12	1	180	405				
		2017*	4	2						
		2014-2025	25-28	1						
12/7 /66	0322	0322-0327	3-4	0.3	(2)		ATS-1	Atlas	0212	70
2 /5 /67	0219	0219-0225	2-7	0.2	184	350	Lunar Orbiter III	Atlas	0117	62
		0225-0233	20-26	0.2	173	380				
		0235*	30	0.3						

Date	Start Time (UT)	Interval	Period (s)	Max. Ampl. Zero-peak (dyn/cm^2)	Az (deg)	Vel. (m/s)	Launch			Signal Travel Time (min)
							Name	Booster	Time (UT)	
3 /23/67	0239	0239-0240	4-8	1.5	187	345	Intelsat II	Delta	0130	69
		0240-0242	8-10	1.0	182	340				
		0242-0247	20-30	0.4						
4 /6 /67	0439	0439-0450	28-33	0.5	176	360	ATS II	Atlas	0323	76
		0448-0451	10-12	0.4						
		0457*	16	0.6	177	450				
7 /1 /67	1422	1422-1443	28-40	0.7	185	405	Navy		1315	67
		1434-1448	12-20	0.4						
7 /14/67	1305	1305-1315	20-30	0.2	192	370	Surveyor IV	Atlas	1153	72
		1309*	15	0.3						
7 /19/67	1545	1545*	1-2	0.4	185	440	Explorer XXXV	Delta	1419	86
8 /1 /67	2346	2346-2352	11-15	0.3	188	345	Lunar Orbiter V	Atlas	2233	73
8 /17/67	2227	2227-2238	22-31	0.2	190	320	Minute Man		2119	68
9 /7 /67	2317	2317-2328	22-28	0.8	188	360	Biosat II	Delta	2204	73
		2330*	20	1.2	191	360				
		2339*	21	0.4	192	410				
9 /8 /67	0906	0906-0911	4-7	0.6	198	360	Surveyor V	Atlas	0757	69
		0909-0920	19-30	0.8	189	380				
		0926*	24	1.1	183	465				
9 /28/67	0159	0159-0206	5-7	0.1	189	360	Intelsat II	Delta	0045	74
11/6 /67	0040	0040*	5	3.2	188	340	ATS III	Atlas	2337	63
		0040-0046	2-4	2.5	186	345				
11/7 /67	0840	0840-0847	3-6	0.8	187	360	Surveyor VI	Atlas	0739	61
		0845-0853	22-27	0.6	173	360				
		0859*	33	0.4	174	425				
11/9 /67	1302	1302-1307	3-5	1.0	179	370	Apollo IV	Saturn	1200	62
		1307-1313	10-15	12.	187	355				
		1315-1320	38-52	6.	176	415				
1 /22/68	2349	2349-2354	3-6	0.9	182	355	Apollo V	Saturn	2248	61
		2354-2357	10-12	2.1	193	345				
		2357	4-5	4.5						
		2357-2359	3-5	1.1						
		2359-0006	14-20	1.0						
		0006-0009	33-41	1.3						
8 /10/68	2341	2341-2350	3-5	0.4	192	360	ATS IV	Atlas	2233	68
		2350-0002	11-15	0.3						
10/11/68	1606	1606-1610	3-4	0.4	192	355	Apollo VII	Saturn	1503	63
		1610-1615	6-8	2.3						
		1615-1620	9-16	1.0	191	370				
		1620-1630	33-40	0.8						
12/19/68	0144	0144-0149	13-18	0.4	190	360	Intelsat III	Delta	0032	72
		0145-0153	4-7	0.4						
		0149*	10	0.9						
		0149-0158	22-33	0.4						
		0206*	40	0.6	199	410				

Date	Start Time (UT)	Interval	Period (s)	Max. Ampl. Zero-peak (dyn/cm^2)	Az (deg)	Vel. (m/s)	Launch			Signal Travel Time (min)
							Name	Booster	Time (UT)	
12/21/68	1355	1355-1403	3-8	1.4	189	345	Apollo VIII	Saturn	1251	64
		1358-1403	10-18	1.6						
		1401-1406	22-28	0.4	185	360				
3 /3 /69	1705	1705-1709	3-9	6.7	189	330	Apollo IX	Saturn	1600	65
		1716*	31	8.1	191	410				
5 /22/69	0316	0316-0322	8-20	0.6						
		0322-0337	19-26	0.6	194	345	Intelsat III	Delta	0200	76
7 /16/69	1431	1431-1443	2-5	2.2	173	340	Apollo XI	Saturn	1332	59
		1443-1446	15-30	0.8						
		1446-1500	10-20	1.3	199	360				
		1500*	35	3.1	202	400				

* Pulse

(1) Amplitude uncertain because difficulties with noise reducing array.

(2) Only two channels operational.